

Thermodynamic guidelines for the prediction of hydrogen storage reactions and their application to destabilized hydride mixtures

Donald J. Siegel,¹ C. Wolverton,^{1,*} and V. Ozoliņš²¹*Ford Motor Company, MD1170/RIC, Dearborn, Michigan 48121, USA*²*Department of Materials Science and Engineering, University of California, Los Angeles, California 90095, USA*

(Received 13 October 2006; revised manuscript received 16 September 2007; published 4 October 2007)

We propose a set of thermodynamic guidelines aimed at facilitating more robust screening of hydrogen-storage reactions. The utility of the guidelines is illustrated by reassessing the validity of reactions recently proposed in the literature and through vetting a list of more than 20 candidate reactions based on destabilized LiBH_4 and $\text{Ca}(\text{BH}_4)_2$ borohydrides. Our analysis reveals several reactions having both favorable thermodynamics and relatively high hydrogen densities (ranging from 5 to 9 wt % H_2 and 85 to 100 g H_2/l), and it demonstrates that chemical intuition alone is not sufficient to identify valid reaction pathways.

DOI: [10.1103/PhysRevB.76.134102](https://doi.org/10.1103/PhysRevB.76.134102)

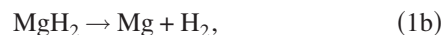
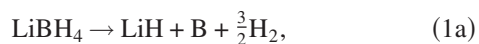
PACS number(s): 68.43.Bc, 64.70.Hz, 82.60.Cx, 84.60.-h

I. INTRODUCTION

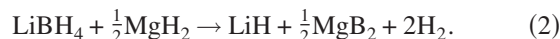
The potential of emerging technologies such as fuel cells (FCs) and photovoltaics for environmentally benign power generation has sparked renewed interest in the development of novel materials for high-density energy storage. For mobile applications such as in the transportation sector, the demands placed upon energy storage media are especially stringent¹ as the leading candidates to replace fossil-fuel-powered internal combustion engines (ICEs)—proton exchange membrane FCs and hydrogen-powered ICEs (H_2 -ICEs)—rely on H_2 as a fuel. Although H_2 has about three times the energy density of gasoline by weight, its volumetric density, even when pressurized to 10 000 psi, is roughly six times less than that of gasoline. Consequently, safe and efficient storage of H_2 has been identified² as one of the key scientific obstacles to realizing a transition to H_2 -powered vehicles.

Perhaps the most promising approach to achieving the high H_2 densities needed for mobile applications is via absorption in solids.³ Metal hydrides such as LaNi_5H_6 have long been known to reversibly store hydrogen at volumetric densities surpassing that of liquid H_2 , but their considerable weight results in gravimetric densities that are too low for lightweight applications.⁴ Accordingly, recent efforts^{5–9} have increasingly focused on low- Z complex hydrides, such as metal borohydrides $M(\text{BH}_4)_n$, where M represents a metallic cation, as borohydrides have the potential to store large quantities of hydrogen (up to 18.5 wt % in LiBH_4). Nevertheless, the thermodynamics of H_2 desorption from known borohydrides are generally not compatible with the temperature-pressure conditions of FC operation; for example, in LiBH_4 , strong hydrogen-host bonds result in desorption temperatures in excess of 300 °C.⁶ Thus, the suitability of LiBH_4 and other stable hydrides as practical H_2 -storage media will depend upon the development of effective destabilization schemes.

Building on earlier work by Reilly and Wiswall¹⁰, Vajo *et al.*¹¹ recently demonstrated that LiBH_4 can be destabilized by mixing with MgH_2 . In isolation, the decomposition of these compounds proceeds according to



yielding 13.6 and 7.6 wt % H_2 , respectively, at temperatures above 300 °C. The high desorption temperatures are consistent with the relatively high enthalpies of desorption: $\Delta H \sim 67$ (LiBH_4) and ~ 70 (MgH_2) kJ/(mol H_2).^{11,12} By mixing LiBH_4 with MgH_2 , ΔH for the combined reaction can be decreased below those of the isolated compounds due to the exothermic formation enthalpy of MgB_2 ,



That is, formation of the MgB_2 product *stabilizes* the dehydrogenated state in Eq. (2) relative to that of Eq. (1), thereby *destabilizing* both LiBH_4 and MgH_2 . By adopting this strategy, measured isotherms for the $\text{LiBH}_4 + \frac{1}{2}\text{MgH}_2$ mixture over 315–400 °C exhibited a 25 kJ/mol H_2 decrease in ΔH relative LiBH_4 alone, with an approximately tenfold increase in equilibrium H_2 pressure.¹¹ In addition, the hydride mixture was shown to be reversible with a density of 8–10 wt % H_2 .¹¹ Nevertheless, the extrapolated temperature $T=225$ °C at which $P_{\text{H}_2}=1$ bar is still too high for mobile applications and suggests that *additional* destabilization is necessary.

The concept of thermodynamic destabilization appears to offer new opportunities for accessing the high H_2 content of strongly bound hydrides. However, the large number of known hydrides suggests that experimentally testing all the possible combinations of known compounds would be impractical; thus, a means for rapidly screening for high-density H_2 -storage reactions with appropriate thermodynamics¹³ would be of great value.³³ Toward these ends, here we employ first-principles calculations to identify H_2 -storage reactions with favorable temperature-pressure characteristics based on destabilizing LiBH_4 and $\text{Ca}(\text{BH}_4)_2$ (Ref. 9) by mixing with selected metal hydrides. Our goal is to determine whether additional destabilization of LiBH_4 and $\text{Ca}(\text{BH}_4)_2$ —beyond that demonstrated¹¹ with $\text{LiBH}_4/\text{MgH}_2$ —is possible by exploiting the exothermic formation enthalpies of the metal borides. We focus specifically on thermodynamic issues since appropriate thermodynamics is a necessary condition for any viable storage material, and thermodynamic properties are not easily altered. While kinet-

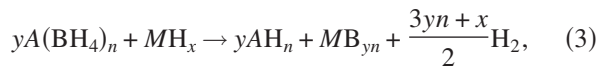
ics must also be considered, catalysts and novel synthesis routes have been shown to be effective at improving reversibility and the rates of H_2 uptake or release.¹⁴ By screening through ~ 20 distinct reactions, we identify four destabilized mixtures having favorable Gibbs free energies of desorption in conjunction with high gravimetric (5–9 wt %) and volumetric (85–100 g H_2 /l) storage densities. The predicted reactions present new avenues for experimental investigation and illustrate that compounds with low gravimetric densities (i.e., transition metal hydrides) may yield viable H_2 -storage solutions when mixed with lightweight borohydrides. An advantage of the present approach is that it relies only on known compounds with established synthesis routes, in contrast to other recent studies which have proposed H_2 -storage reactions based on materials which have yet to be synthesized.^{15–19}

An additional distinguishing feature of this study is the development of a set of thermodynamic guidelines aimed at facilitating more robust predictions of hydrogen-storage reactions. The guidelines are used to vet the present set of candidate reactions and to illustrate how other reactions recently reported in the literature¹³ are thermodynamically unrealistic. In total, this exercise reveals some of the common pitfalls that may arise when attempting to simply “guess” at reaction mechanisms.

II. METHODOLOGY

Our first-principles calculations were performed using a plane-wave-projector augmented wave method (VASP)^{20,21} based on the generalized gradient approximation²² to density functional theory. All calculations employed a plane-wave cutoff energy of 400 eV, and k -point sampling was performed on a dense grid with an energy convergence of better than 1 meV per supercell. Internal atomic positions and external cell shape/volume were optimized to a tolerance of better than 0.01 eV/Å. Thermodynamic functions were evaluated within the harmonic approximation,²³ and normal-mode vibrational frequencies were evaluated using the so-called direct method on expanded supercells.^{24–27} Further information regarding the details and experimental validation of our calculations can be found elsewhere.^{25–27}

Our search for high-density H_2 -storage reactions is based on a series of candidate reactions that are analogous to Eq. (2),



where $A=Li$ or Ca [$n=1$ (2) for Li (Ca)], M represents a metallic element, and coefficients x and y are selected based on the stoichiometries of known hydrides MH_x and borides MB_{yn} . To maximize gravimetric density, we limit M to relatively lightweight elements near the top of the Periodic Table. In the case of $A=Li$, the enthalpy of Eq. (3) per mol H_2 can be expressed as

$$\Delta H = \frac{2}{3y+x} \left[\frac{3y}{2} \Delta H^{LiBH_4} + \frac{x}{2} \Delta H^{MH_x} - \Delta H^{MB_y} \right], \quad (4)$$

where ΔH^i are the desorption (formation) enthalpies of the respective hydrides (borides) per mol H_2 (M). Thus, ΔH for the destabilized $LiBH_4$ reaction is simply an average of the hydride desorption enthalpies, less the enthalpy of boride formation.

III. RESULTS

Table I lists theoretical H_2 densities and calculated dehydrogenation enthalpies and entropies for several potential H_2 -storage reactions. Reactions 1–22 enumerate the candidate reactions, while reactions 23–27 are included in order to validate the accuracy of our predictions by comparing with experimentally measured enthalpies^{11,12,29} and previous first-principles results¹³ (shown in parentheses). Turning first to the reactions from experiment (24–27), it is clear that the calculated $T=300$ K enthalpies are generally in good agreement with the measured data. As mentioned above, reaction 24 was studied by Vajo *et al.*¹¹ [see Eq. (2)]. Our calculated enthalpy of 50.4 kJ/mol H_2 overestimates the experimental value by ~ 10 kJ/mol. However, since the experimental measurements were made at temperatures ($T=315$ – 400 °C) above the $LiBH_4$ melting point ($T_m=268$ °C),⁶ and our calculations are with respect to the ground state $Pnma$ crystal structure,⁶ we expect $\Delta H^{calc}(Pnma) > \Delta H^{expt}(liquid)$ due to the higher enthalpy of the liquid state.

We begin our discussion of the candidate reactions by commenting on the vibrational contributions (ΔS_{vib}) of the solid state phases to the total dehydrogenation entropy ΔS . Based on the notion that ΔS is largely due to the entropy of H_2 [$\Delta S \approx S_0^{H_2} \approx 130$ J/(mol K) at 300 K], a dehydrogenation enthalpy in the approximate range of 20–50 kJ/mol H_2 would yield desorption pressures/temperatures that are consistent with the operating conditions of a FC.³ However, as shown in the last column of Table I, the calculated ΔS_{vib} are not negligible (up to 21%) in comparison to $S_0^{H_2}$, calling into question the assumption $\Delta S \approx S_0^{H_2}$ and the guideline $\Delta H = 20$ – 50 kJ/mol H_2 . This suggests that a precise determination of the temperature-pressure characteristics of a given desorption reaction requires an evaluation of the change in Gibbs free energy [$\Delta G(T)$], accounting explicitly for the effects of temperature and ΔS_{vib} , as done below.

A. Thermodynamic guidelines

A key concern when attempting to predict favorable hydrogen-storage reactions is to ensure that the thermodynamically preferred reaction pathway has been identified. This is a nontrivial task, and our experience has shown that intuition alone is not sufficient to correctly identify realistic reactions involving multicomponent systems.²⁶ In this regard, several of the reactions in Table I (denoted by *) are noteworthy as they illustrate the difficulties that may arise when “guessing” at reactions. For example, all of the candidate reactions are written as simple, single-step reactions.

TABLE I. H_2 densities and calculated thermodynamic quantities for candidate H_2 -storage reactions. Units are J/K mol H_2 for ΔS_{vib} and kJ/mol H_2 for ΔE and ΔH ; column 7 refers to the temperature at which $P_{H_2}=1$ bar. Reactions denoted with a * will not proceed as written (see text). The enthalpies of reactions 24–27 have been measured in prior experiments and are included here (in parentheses) to validate the accuracy of our calculations. For comparison, system-level targets for gravimetric and volumetric densities are cited in the bottom row (Ref. 28).

Rxn. No.	Reaction	wt. % (kg H_2 /kg)	Vol. density (g H_2 /l)	ΔE	$\Delta H^{T=300 \text{ K}}$	$T, P=1 \text{ bar}$ ($^{\circ}\text{C}$)	$\Delta S_{\text{vib}}^{T=300 \text{ K}}$
1*	$4\text{LiBH}_4 + 2\text{AlH}_3 \rightarrow 2\text{AlB}_2 + 4\text{LiH} + 9\text{H}_2$	12.4	106	54.8	39.6	83	-18.4
2	$2\text{LiBH}_4 + \text{Al} \rightarrow \text{AlB}_2 + 2\text{LiH} + 3\text{H}_2$	8.6	80	77.0	57.9	277	-26.9
3*	$4\text{LiBH}_4 + \text{MgH}_2 \rightarrow \text{MgB}_4 + 4\text{LiH} + 7\text{H}_2$	12.4	95	68.2	51.8	206	-23.3
4*	$2\text{LiBH}_4 + \text{Mg} \rightarrow \text{MgB}_2 + 2\text{LiH} + 3\text{H}_2$	8.9	76	65.9	46.4	170	-29.4
5	$2\text{LiBH}_4 + \text{TiH}_2 \rightarrow \text{TiB}_2 + 2\text{LiH} + 4\text{H}_2$	8.6	103	21.4	4.5		-23.3
6	$2\text{LiBH}_4 + \text{VH}_2 \rightarrow \text{VB}_2 + 2\text{LiH} + 4\text{H}_2$	8.4	105	24.7	7.2	-238	-21.7
7	$2\text{LiBH}_4 + \text{ScH}_2 \rightarrow \text{ScB}_2 + 2\text{LiH} + 4\text{H}_2$	8.9	99	48.8	32.6	26	-21.4
8*	$2\text{LiBH}_4 + \text{CrH}_2 \rightarrow \text{CrB}_2 + 2\text{LiH} + 4\text{H}_2$	8.3	109	33.9	16.4	-135	-19.2
9*	$2\text{LiBH}_4 + 2\text{Fe} \rightarrow 2\text{FeB} + 2\text{LiH} + 3\text{H}_2$	3.9	76	32.7	12.8	-163	-24.6
10	$2\text{LiBH}_4 + 4\text{Fe} \rightarrow 2\text{Fe}_2\text{B} + 2\text{LiH} + 3\text{H}_2$	2.3	65	21.6	1.2		-24.4
11	$2\text{LiBH}_4 + \text{Cr} \rightarrow \text{CrB}_2 + 2\text{LiH} + 3\text{H}_2$	6.3	84	50.9	31.7	25	-23.8
12	$\text{Ca}(\text{BH}_4)_2 \rightarrow \frac{2}{3}\text{CaH}_2 + \frac{1}{3}\text{CaB}_6 + \frac{10}{3}\text{H}_2$	9.6	107	57.1	41.4	88	-16.0
13*	$\text{Ca}(\text{BH}_4)_2 + \text{MgH}_2 \rightarrow \text{CaH}_2 + \text{MgB}_2 + 4\text{H}_2$	8.4	99	61.6	47.0	135	-16.2
14*	$2\text{Ca}(\text{BH}_4)_2 + \text{MgH}_2 \rightarrow 2\text{CaH}_2 + \text{MgB}_4 + 7\text{H}_2$	8.5	98	63.6	47.9	147	-17.0
15*	$\text{Ca}(\text{BH}_4)_2 + \text{Mg} \rightarrow \text{CaH}_2 + \text{MgB}_2 + 3\text{H}_2$	6.4	79	60.6	41.9	111	-22.0
16*	$\text{Ca}(\text{BH}_4)_2 + \text{Al} \rightarrow \text{CaH}_2 + \text{AlB}_2 + 3\text{H}_2$	6.3	83	71.7	53.4	200	-19.5
17*	$\text{Ca}(\text{BH}_4)_2 + \text{AlH}_3 \rightarrow \text{CaH}_2 + \text{AlB}_2 + \frac{9}{2}\text{H}_2$	9.1	109	51.2	36.6	39	-13.5
18	$\text{Ca}(\text{BH}_4)_2 + \text{ScH}_2 \rightarrow \text{CaH}_2 + \text{ScB}_2 + 4\text{H}_2$	6.9	102	44.8	29.2	-20	-15.9
19	$\text{Ca}(\text{BH}_4)_2 + \text{TiH}_2 \rightarrow \text{CaH}_2 + \text{TiB}_2 + 4\text{H}_2$	6.7	106	17.4	1.1		-17.7
20	$\text{Ca}(\text{BH}_4)_2 + \text{VH}_2 \rightarrow \text{CaH}_2 + \text{VB}_2 + 4\text{H}_2$	6.6	108	20.8	3.8		-16.2
21*	$\text{Ca}(\text{BH}_4)_2 + \text{CrH}_2 \rightarrow \text{CaH}_2 + \text{CrB}_2 + 4\text{H}_2$	6.5	113	29.9	13.1	-180	-13.6
22	$\text{Ca}(\text{BH}_4)_2 + \text{Cr} \rightarrow \text{CaH}_2 + \text{CrB}_2 + 3\text{H}_2$	5.0	86	45.6	27.2	-38	-16.4
23	$6\text{LiBH}_4 + \text{CaH}_2 \rightarrow \text{CaB}_6 + 6\text{LiH} + 10\text{H}_2$	11.7	93	61.9 (63) ^a	45.4	146	-22.7
24	$2\text{LiBH}_4 + \text{MgH}_2 \rightarrow \text{MgB}_2 + 2\text{LiH} + 4\text{H}_2$	11.6	96	65.6	50.4 (41) ^b	186	-21.7
25	$2\text{LiBH}_4 \rightarrow 2\text{LiH} + 2\text{B} + 3\text{H}_2$	13.9	93	81.4	62.8 (67) ^b	322	-27.1
26	$\text{LiBH}_4 \rightarrow \text{Li} + \text{B} + 2\text{H}_2$	18.5	124	103.5	89.7 (95) ^c	485	-15.3
27	$\text{MgH}_2 \rightarrow \text{Mg} + \text{H}_2$	7.7	109	64.5	62.3	195	1.3
					(65.8–75.2) ^d		
	U.S. DOE system-level targets (2010/2015)	6/9	45/81				

^aReference 13.

^bReference 11.

^cReference 29.

^dReference 12.

While this may seem reasonable given the mechanism proposed in Ref. 11 [Eq. (2)] and its generalization in Eq. (3), as we discuss below, some of these reactions should proceed via multiple-step pathways, with each step having thermodynamic properties that are distinct from the presumed single-step pathway.

We group the examples of how chemical intuition might fail into three categories, and for each class, give a general guideline describing the thermodynamic restriction:

(1) *Reactant mixtures involving “weakly bound” compounds.* We refer here to systems where the enthalpy to decompose one (or more) of the reactant phases is less than the enthalpy of the proposed destabilized reaction; thus, the

weakly bound phase(s) will decompose before (i.e., at a temperature below that which) the destabilized reaction can proceed. Two examples of this behavior can be found in Table I. The first case pertains to reactions 13–16, which, based on their larger enthalpies relative to reaction 12, would appear to “stabilize” $\text{Ca}(\text{BH}_4)_2$. In reality, $\text{Ca}(\text{BH}_4)_2$ will decompose before (with $P_{H_2}=1$ bar at $T=88$ $^{\circ}\text{C}$) any of the higher temperature reactions 13–16 will occur ($T>110$ $^{\circ}\text{C}$), indicating that it is impossible to stabilize a reaction in this manner. Additional examples of this scenario occur in reactions 1, 8, 17, and 21, which involve the metastable AlH_3 and CrH_2 phases. In the case of reaction 1, AlH_3 will decompose first (yielding Al and $\frac{3}{2}\text{H}_2$), followed by reaction of Al with

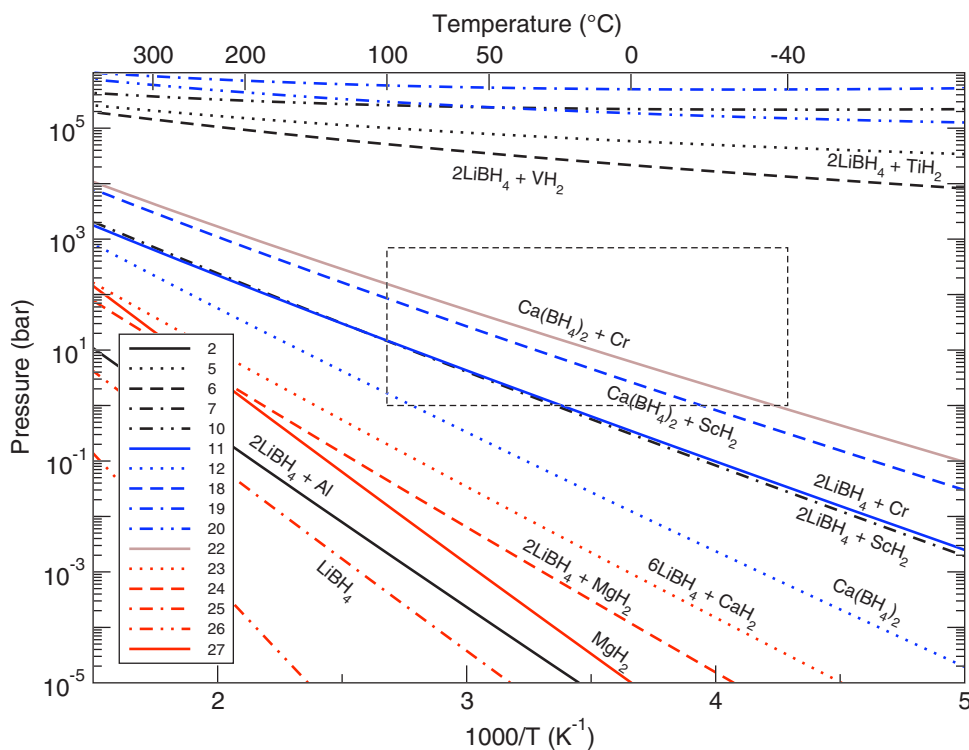
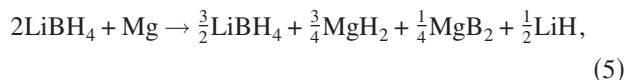


FIG. 1. (Color online) Calculated van't Hoff plot for reactions listed in Table I. The region within the dashed box corresponds to desirable temperatures and pressures for on-board hydrogen storage: $P_{\text{H}_2} = 1 - 700$ bar $T = -40 - 100$ °C.

LiBH_4 (reaction 2). The consequences of this behavior are significant, since although the intended reaction 1 has an enthalpy (~ 40 kJ/mol H_2) in the targeted range, in reality, the reaction will consist of two steps, the first of which has an enthalpy below the targeted range (AlH_3 decomposition), while the second (reaction 2) has an enthalpy above this range. *Guideline 1: The enthalpy of the proposed destabilized reaction must be less than the decomposition enthalpies of the individual reactant phases.*

(2) *Unstable combinations of product or reactant phases.* Reaction 4 illustrates how the seemingly straightforward process of identifying stable reactant and product phases can become unexpectedly complex. Here, the starting mixture of LiBH_4 and Mg is unstable and will undergo the exothermic transformation,



which will consume the available Mg and form MgH_2 . MgH_2 will react endothermically with the remaining LiBH_4 according to reaction 24. The exothermic nature of Eq. (5) can be understood by noting that the enthalpy of reaction 4 (46.4 kJ/mol H_2) is lower than the decomposition enthalpy of MgH_2 , given by reaction 27 (62.3 kJ/mol H_2). Therefore, the total energy can be lowered by transferring hydrogen to the more strongly bound MgH_2 compound. *Guideline 2: If the proposed reaction involves a reactant that can absorb hydrogen (such as an elemental metal), the formation enthalpy of the corresponding hydride cannot be greater in magnitude than the enthalpy of the destabilized reaction.*

(3) *Lower-energy reaction pathways.* Reaction 3, involving a 4:1 mixture of $\text{LiBH}_4:\text{MgH}_2$, as well as the related reaction involving a 7:1 stoichiometry, $7\text{LiBH}_4 + \text{MgH}_2$

$\rightarrow \text{MgB}_7 + 7\text{LiH} + 11.5\text{H}_2$, were recently suggested in Ref. 13, which considered only a single-step mechanism resulting in the formation of MgB_4 and MgB_7 , respectively. Here, we demonstrate that these reactions will not proceed as suggested there due to the presence of intermediate stages with lower energies. In fact, both hypothetical reactions have larger enthalpies [$\Delta E = 69$ (4:1) and 74 (7:1) kJ/mol H_2 (Ref. 13)] than the 2:1 mixture (reaction 24), suggesting that, upon increasing temperature, the 4:1 and 7:1 mixtures will follow a pathway whose initial reaction step is the 2:1 reaction (reaction 24), which will consume all available MgH_2 . Subsequent reactions between unreacted LiBH_4 and newly formed MgB_2 will become thermodynamically feasible at temperatures above that of reaction 24 since their enthalpies exceed 50 kJ/mol H_2 . [Similar behavior is expected for reactions 9 and 10, as the 1:1 mixture of $\text{LiBH}_4:\text{Fe}$ (reaction 9) will initially react in a 1:2 ratio (reaction 10), which has a lower enthalpy.] *Guideline 3: In general, it is not possible to tune the thermodynamics of destabilized reactions by adjusting the molar fractions of the reactants. There is only one stoichiometry corresponding to a single-step reaction with the lowest possible enthalpy; all other stoichiometries will release H_2 in multistep reactions, where the initial reaction is given by the lowest-enthalpy reaction.*³⁴

B. Destabilized reactions

In total, the preceding examples reveal that great care must be taken in predicting hydrogen-storage reactions. Having ruled out the specious reactions, we now discuss the thermodynamics of the remaining reactions. Using the calculated thermodynamic data (Table I) as input to the van't Hoff

equation, $P_{\text{H}_2} = P_0 \exp\left(-\frac{\Delta G}{RT}\right)$, where $P_0 = 1$ bar, Fig. 1 plots the equilibrium H_2 desorption pressures of these reactions as a function of temperature.³⁵ Included in the plot is a rectangle delineating desirable temperature and pressure ranges for H_2 storage: -40 – 100 °C and 1 – 700 bar.

As expected, our van't Hoff plot confirms that the experimental reactions having large dehydrogenation enthalpies (reactions 24–27) yield pressures $P \ll 1$ bar even at elevated temperatures. On the other hand, some of the candidate reactions, for example, 5 and 19, readily evolve H_2 at very low temperatures (consistent with their low enthalpies) and are therefore too weakly bound for practical, reversible on-board storage. However, the candidate reactions involving mixtures with ScH_2 (Ref. 36) [reactions 7 (Ref. 37) and 18] and Cr (reactions 11 and 22) desorb H_2 in P - T regimes that strongly intersect the window of desirable operating conditions. These reactions have room-temperature enthalpies in the range of 27 – 33 kJ/mol H_2 , relatively high H_2 densities (5 – 8.9 wt % H_2 and 85 – 100 g H_2/l), and achieve $P_{\text{H}_2} = 1$ bar at moderate temperatures ranging from -38 to 26 °C. Thus, via a first-principles approach of rapid screening through a large number of candidate reactions, and the careful use of thermodynamic considerations to eliminate unstable or multistep reactions, we predict here several reactions with attributes

that surpass the state-of-the-art for reversible, low-temperature storage materials.

IV. CONCLUSION

In conclusion, using first-principles free energy calculations, we have demonstrated that further significant destabilization of the strongly bound LiBH_4 and $\text{Ca}(\text{BH}_4)_2$ borohydrides is possible, and we identify several high H_2 -density reactions having thermodynamics compatible with the operating conditions of mobile H_2 -storage applications. Unlike other recent predictions, the proposed reactions utilize only known compounds with established synthesis routes and can therefore be subjected to immediate experimental testing. In addition, we provide guidance to subsequent efforts aimed at predicting H_2 -storage materials by illustrating common pitfalls that arise when attempting to guess at reaction mechanisms, and by suggesting a set of thermodynamic guidelines to facilitate more robust predictions.

ACKNOWLEDGMENTS

V.O. thanks the U.S. DOE for financial support under Grants No. DE-FG02-05ER46253 and No. DE-FC36-04GO14013.

*Present address: Department of Materials Science and Engineering, Northwestern University, Evanston, IL 60208.

¹F. E. Pinkerton and B. G. Wicke, *Ind. Phys.* **10**, 20 (2004).

²G. W. Crabtree, M. S. Dresselhaus, and M. V. Buchanan, *Phys. Today* **57**(12), 39 (2004).

³L. Schlapbach and A. Züttel, *Nature (London)* **414**, 353 (2001).

⁴G. Sandrock, *J. Alloys Compd.* **293-295**, 877 (1999).

⁵J.-P. Soulie, G. Renaudin, R. Cerny, and K. Yvon, *J. Alloys Compd.* **346**, 200 (2002).

⁶A. Züttel, S. Rentsch, P. Fischer, P. Wenger, P. Sudan, P. Mauron, and C. Emmenegger, *J. Alloys Compd.* **356-357**, 515 (2003).

⁷Y. Nakamori, K. Miwa, A. Ninomiya, H. Li, N. Ohba, S. Towata, A. Züttel, and S. Orimo, *Phys. Rev. B* **74**, 045126 (2006).

⁸Z. Łodziana and T. Vegge, *Phys. Rev. Lett.* **93**, 145501 (2004).

⁹K. Miwa, M. Aoki, T. Noritake, N. Ohba, Y. Nakamori, S. I. Towata, A. Züttel, and S. I. Orimo, *Phys. Rev. B* **74**, 155122 (2006).

¹⁰J. J. Reilly and R. H. Wiswall, *Inorg. Chem.* **7**, 2254 (1968).

¹¹J. J. Vajo, S. L. Skeith, and F. Mertens, *J. Phys. Chem. B* **109**, 3719 (2005).

¹²*Phase Diagrams of Binary Hydrogen Alloys*, edited by F. D. Manchester (ASM, Materials Park, OH, 2000).

¹³S. V. Alapati, J. K. Johnson, and D. S. Sholl, *J. Phys. Chem. B* **110**, 8769 (2006).

¹⁴B. Bogdanović and M. Schwickardi, *J. Alloys Compd.* **253-254**, 1 (1997).

¹⁵W.-Q. Deng, X. Xu, and W. A. Goddard, *Phys. Rev. Lett.* **92**, 166103 (2004).

¹⁶Y. Zhao, Y.-H. Kim, A. C. Dillon, M. J. Heben, and S. B. Zhang, *Phys. Rev. Lett.* **94**, 155504 (2005).

¹⁷T. Yildirim and S. Ciraci, *Phys. Rev. Lett.* **94**, 175501 (2005).

¹⁸H. Lee, W. I. Choi, and J. Ihm, *Phys. Rev. Lett.* **97**, 056104 (2006).

¹⁹Q. Sun, P. Jena, Q. Wang, and M. Marquez, *J. Am. Chem. Soc.* **128**, 9741 (2006).

²⁰G. Kresse and J. Furthmüller, *Phys. Rev. B* **54**, 11169 (1996).

²¹P. E. Blöchl, *Phys. Rev. B* **50**, 17953 (1994).

²²J. P. Perdew, J. A. Chevary, S. H. Vosko, K. A. Jackson, M. R. Pederson, D. J. Singh, and C. Fiolhais, *Phys. Rev. B* **46**, 6671 (1992).

²³D. C. Wallace, *Thermodynamics of Crystals* (Wiley, New York, 1972).

²⁴S. Wei and M. Y. Chou, *Phys. Rev. Lett.* **69**, 2799 (1992).

²⁵C. Wolverton, V. Ozoliņš, and M. Asta, *Phys. Rev. B* **69**, 144109 (2004).

²⁶D. J. Siegel, C. Wolverton, and V. Ozoliņš, *Phys. Rev. B* **75**, 014101 (2007).

²⁷C. Wolverton and V. Ozolins, *Phys. Rev. B* **75**, 064101 (2007).

²⁸S. Satyapal, J. Petrovic, C. Read, G. Thomas, and G. Ordaz, *Catal. Today* **120**, 246 (2007).

²⁹M. W. Chase, Jr., *NIST-JANAF Thermochemical Tables*, 4th ed. (American Chemical Society, Washington, DC 1998).

³⁰A. Sudik (private communication).

³¹D. J. Siegel, V. Ozolins, and C. Wolverton, *Phys. Rev. B* (unpublished).

³²S. V. Alapati, J. K. Johnson, and D. S. Sholl, *Phys. Chem. Chem. Phys.* **9**, 1438 (2007).

³³Experimental testing of hydrogen-storage materials—many of which are air sensitive—can be a slow, painstaking process. For example, an equilibrium measurement of the extent of hydrogen

desorption or uptake at a single temperature may require several *months* to complete in kinetically hindered materials (Ref. 30). In contrast, the first-principles thermodynamic calculations presented here (encompassing more than 20 unique reactions) were completed in 2–3 weeks.

³⁴This discussion assumes that the entropies of all competing reaction pathways are similar. Our results in Table I show that this is generally not the case; generalization of the above guidelines to

the free energies is straightforward and will be presented elsewhere (Ref. 31).

³⁵We neglect the LiBH_4 structural transition at $T_s \sim 108^\circ\text{C}$ ⁵, which should reduce the slope of the data in Fig. 1 for $T > T_s$.

³⁶It should be noted that the high cost of Sc may preclude its use in practical applications.

³⁷This reaction was also reported in Ref. 32.